

## Measurement of the cosmic ray energy spectrum in the 2nd knee region with the TALE-SD array

---

Ichiro Komae<sup>a,\*</sup> for the Telescope Array collaboration

<sup>a</sup>Graduate School of Science, Osaka Metropolitan University,  
3-3-138, Sugimoto, Sumiyoshi-ku, Osaka, 558-8585, Japan

E-mail: [i.komae@cosmicray-ocu.jp](mailto:i.komae@cosmicray-ocu.jp)

The Telescope Array Low-energy Extension (TALE) experiment observes cosmic rays with 10 atmospheric fluorescence telescopes and an array of 80 surface detectors (SDs) distributed over an area of 21 km<sup>2</sup>. The SD array consists of 40 SDs spaced at 400 m and 40 SDs spaced at 600 m. One of the goals of TALE-SD is to observe cosmic rays with energies down to 10<sup>16.5</sup> eV to resolve the origin of the second knee and the energy of a galactic-extragalactic transition. The TALE-SD was completed in February 2018 and has been in continuous operation since then. In this work, we present the cosmic ray energy spectrum from the data recorded by the TALE-SD array from October 2nd, 2019 to September 28th, 2022.

38th International Cosmic Ray Conference (ICRC2023)  
26 July - 3 August, 2023  
Nagoya, Japan

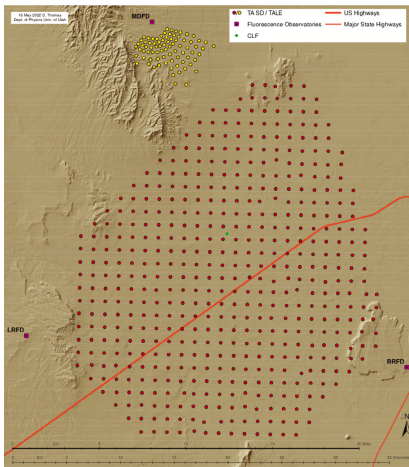


---

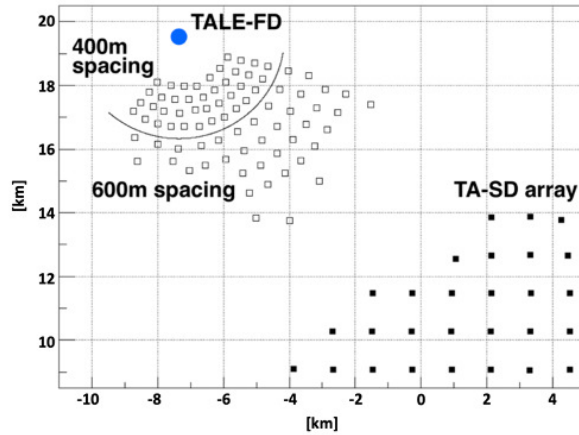
\*Speaker

## 1. Introduction

The Telescope Array (TA) experiment measures extremely high energy cosmic rays [1]. TA is located in the western desert of Utah, USA and has been collecting data since March 2007. It includes a surface detector (SD) array and three fluorescence detector (FD) stations which measure properties of extensive air showers induced by high energy cosmic rays. The TA-SD array consists of 507 plastic scintillation detectors deployed at 1.2 km intervals, covering an area of approximately 700 km<sup>2</sup> [2]. The Black Rock Mesa (BRFD) and Long Ridge (LRFD) stations are composed of 12 telescopes which view 3° to 33° in elevation and 108° in azimuth [3]. The Middle Drum (MDFD) station consists of 14 telescopes, covering 3° to 31° in elevation and an azimuth range of 112° [4]. A map of the TA and TALE site is shown in Figure 1a.



(a) Map of the TA and TALE site.



(b) Map of the TALE site.

**Figure 1:** Maps of the TA and TALE detectors. (a) : Locations of the TA-SDs are shown as red points and the locations of the three TA-FD stations are indicated by the magenta squares. Locations of the TALE-SDs are shown as yellow points. (b) : A map of the TALE site. Locations of the TALE-SDs are shown as open squares and the location of the TALE-FD station is shown as a blue circle. Locations of the TA-SDs are shown as black squares. The area closest to the TALE-FD station has 40 SDs with a spacing of 400 m, and the outer area has 40 SDs with a spacing of 600 m. The TALE-SD array is arranged in a fan shape instead of a grid shape to optimize the hybrid observation with TALE-FD. The TALE-FD consists of 10 telescopes viewing the sky above the MDFD from 31° to 59° in elevation.

The Telescope Array Low-energy Extension (TALE) experiment observes cosmic rays with 10 FDs and an array of 80 SDs distributed over an area of 21 km<sup>2</sup>. The SD array consists of 40 SDs spaced at 400 m and 40 SDs spaced at 600 m. The 10 FDs were installed at the Middle Drum site, observing elevation angles from 31° to 59° [5] above the original TA telescopes. The layout of the TALE surface detectors is shown in Figure 1b.

One of the goals of TALE-SD is to observe cosmic rays with energies down to 10<sup>16.5</sup> eV to resolve the origin of the second knee and the energy of a galactic-extragalactic transition. TALE-SD was completed in February 2018 and has been in continuous operation since then. In this work, we present the cosmic ray energy spectrum from the data recorded by the TALE-SD array from October 2nd, 2019 to September 28th, 2022.

## 2. Event reconstruction and selection

Approximately three years of data recorded between October 2nd, 2019 and September 28th, 2022 were analyzed for measuring the cosmic ray spectrum with the TALE-SD array. In this analysis, cosmic ray events were reconstructed as follows [6].

The geometric parameters of the event were reconstructed using the following function:

$$\tau = \left(8 \times 10^{-10}\right) a(\theta) \left(1.0 + \frac{r}{30}\right)^{1.5} \left(\frac{\rho}{\text{m}^{-2}}\right)^{-0.5} [\text{s}]. \quad (1)$$

As shown in Figure 2,  $\tau$  is the delay in particle arrival time from the shower plane,  $r$  is the distance from the shower axis to the SD and  $\rho$  is the particle number density.

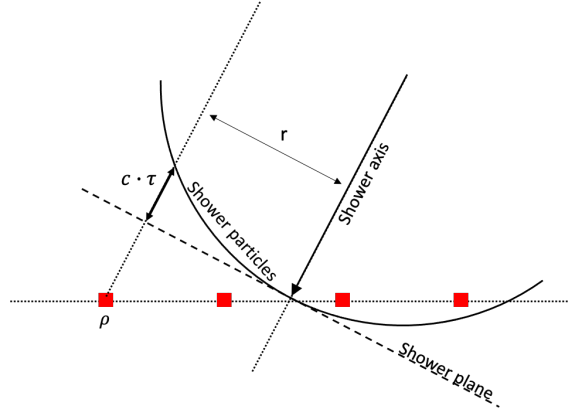


**Figure 2:** Schematic diagram of an air shower and TALE-SDs. The red squares are TALE-SDs, the dashed line is the shower plane and the black curve shows the positions of the shower particles.  $\tau$  is the delay in particle arrival time from the shower plane,  $c$  is the light speed,  $r$  is the distance from the shower axis to the SD and  $\rho$  is the particle number density recorded by the SD.

$a(\theta)$  is the curvature of the air shower plane and is given by

$$a(\theta) = \begin{cases} 3.3836 - 0.01848\theta & (\theta < 25^\circ) \\ c_0 + c_1\theta + c_2\theta^2 + c_3\theta^3 & (25^\circ \leq \theta \leq 35^\circ), \\ \exp(-3.2 \times 10^{-2}\theta + 2.0) & (35^\circ < \theta) \end{cases}, \quad (2)$$

$$c_0 = -7.76168 \times 10^{-2}, \quad c_1 = 2.99113 \times 10^{-1},$$

$$c_2 = -8.79358 \times 10^{-3}, \quad c_3 = 6.51127 \times 10^{-5}.$$

These equations were obtained by Linsley and parameterized by zenith angle  $\theta$  for the TA experiment [7][8].

Next, the particle density obtained from each detector is fitted with the following lateral distribution function  $f_{\text{LDF}}(r)$  from the Akeno Giant Air Shower Array (AGASA) experiment [9],

$$f_{\text{LDF}}(r) = A \left(\frac{r}{91.6 \text{ m}}\right)^{-1.2} \left(1.0 + \frac{r}{91.6 \text{ m}}\right)^{-\eta(\theta)+1.2} \left(1 + \left(\frac{r}{1000 \text{ m}}\right)^2\right)^{-0.6} [\text{m}^{-2}] \quad (3)$$

$$\eta(\theta) = 3.97 - 1.79(\sec \theta - 1)$$

where  $r$  is the distance from the shower axis to the SD,  $\theta$  is the zenith angle and  $A$  is the scale factor.

TALE-SD determines the energy of observed air showers using the reconstructed zenith angle  $\theta$ , the particle number density at 600 m from the shower axis  $S_{600}$  and an energy estimation table obtained from Monte Carlo simulations. A preliminary version of the TALE-SD energy estimation table is shown in Figure 3. This result assumes a pure proton composition, and is made using

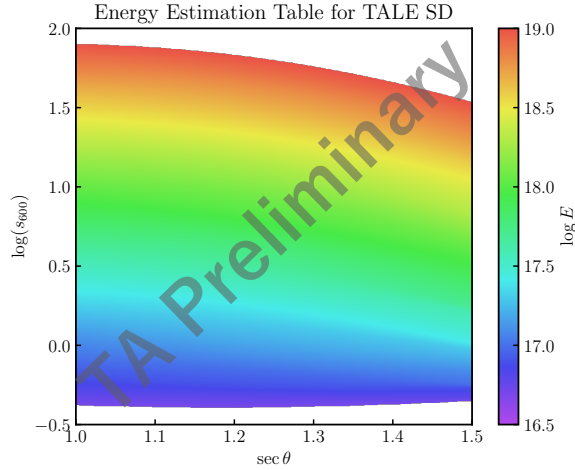


**Figure 3:** Energy Estimation Table for TALE-SD array. This energy estimation table assumes a pure proton. The energy range that can be estimated using this is from  $10^{16.7}$  eV to  $10^{19.0}$  eV.

the quality cuts shown below in Table 1. When calculating the spectrum a more stringent zenith angle cut, also shown in Table 1, was applied to ensure good resolution and data/Monte Carlo comparisons. As shown in Figure 4, the primary energies obtained from this analysis and the TALE-Hybrid analysis are consistent [10][11].

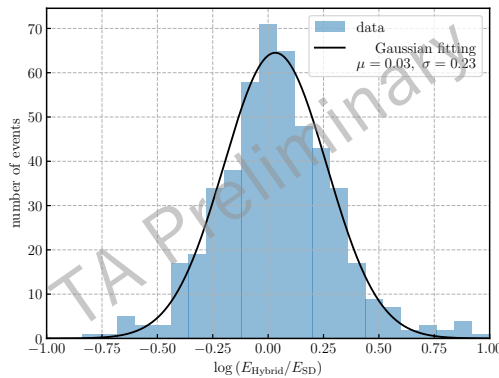


**Figure 4:** Comparison of the primary energy obtained from this analysis with the primary energy obtained from the TALE-Hybrid analysis. The black line is the result of a Gaussian fit to the histogram.

### 3. Monte Carlo simulation

We generated air showers using the CORSIKA-based Monte Carlo simulation code developed for the TA experiments [12]. These simulations first simulate an air shower using the hadronic interaction model QGSJETII-04 [13], followed by the detector response of the TALE-SD, which is calculated using GEANT4 [14]. In this analysis, the primary particle is assumed to be a proton, and the air showers are generated with energies from  $10^{16.65}$  eV to  $10^{18.95}$  eV where  $dN/dE$  is proportional to  $E^{-3.3}$ . The azimuth angle was uniformly selected from  $0^\circ$  to  $360^\circ$ , the zenith angle was sampled from a  $\cos \theta \sin \theta$  distribution between  $0^\circ$  to  $65^\circ$ , giving an equal number of events per solid angle, and the core positions were uniformly selected within a 5.5 km radius circle that completely includes the TALE-SD array, as shown in Figure 5.

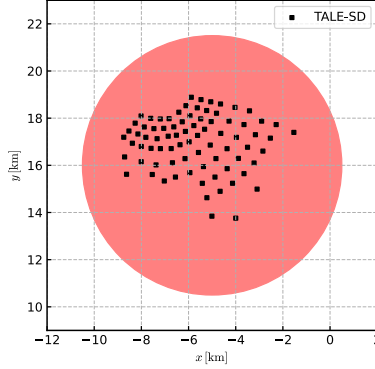


**Figure 5:** Distribution of the shower core positions. The shower core positions were uniformly selected within a 5.5 km radius circle that completely includes the TALE-SD array.

Comparing the reconstruction to the Monte Carlo simulated values estimates the analysis resolution. Figure 6 shows the reconstruction performance. The energy resolution is 25% at  $10^{16.7}$  eV and 15% at  $10^{18.9}$  eV. The angular resolution is  $3^\circ$  at  $10^{16.7}$  eV and almost  $1^\circ$  at  $10^{18.9}$  eV.

To check whether the Monte Carlo simulation reasonably simulated the TALE-SD data, the distribution of the measurable parameters were plotted. Figure 7 shows data and Monte Carlo comparisons for primary energy, zenith angle, azimuthal angle,  $S_{600}$ , the shower core position in  $x$  and the shower core position in  $y$ . The data is shown as black points with error bars. The Monte Carlo is represented by the blue histogram. The Monte Carlo simulation is a good representation of the data. The two are consistent.

**Table 1:** Quality Cuts Applied in this study.

Variable	cut condition	Variable	cut condition
# of SDs	$\geq 5$	$\chi_{\text{Geom}}^2 / \text{d.o.f}$	$\leq 4$
zenith angle [ $^\circ$ ]	$\leq 55^\circ$ (To create Energy Estimation Table)	$\chi_{\text{LDF}}^2 / \text{d.o.f}$	$\leq 2$
	$\leq 45^\circ$ (To analyze data)	$(\sigma_\theta^2 + \sin^2 \theta \sigma_\phi^2)^{1/2}$ [ $^\circ$ ]	$\leq 2.5^\circ$
$D_{\text{border}}$ [m]	$\sim 100$ m	$\sigma_{S600} / S600$	$\leq 0.25$

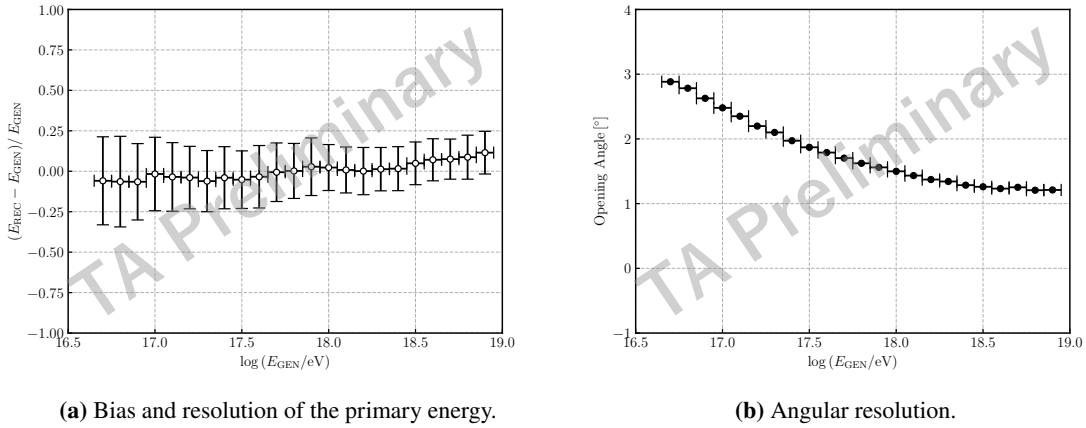


**Figure 6:** Result obtained by Monte Carlo simulation. (a): Bias (open circles) and  $\pm 1\sigma$  resolution (error bars) of the primary energy obtained by Gaussian fitting. (b): Opening angle at 68% of the number of events at a given energy.

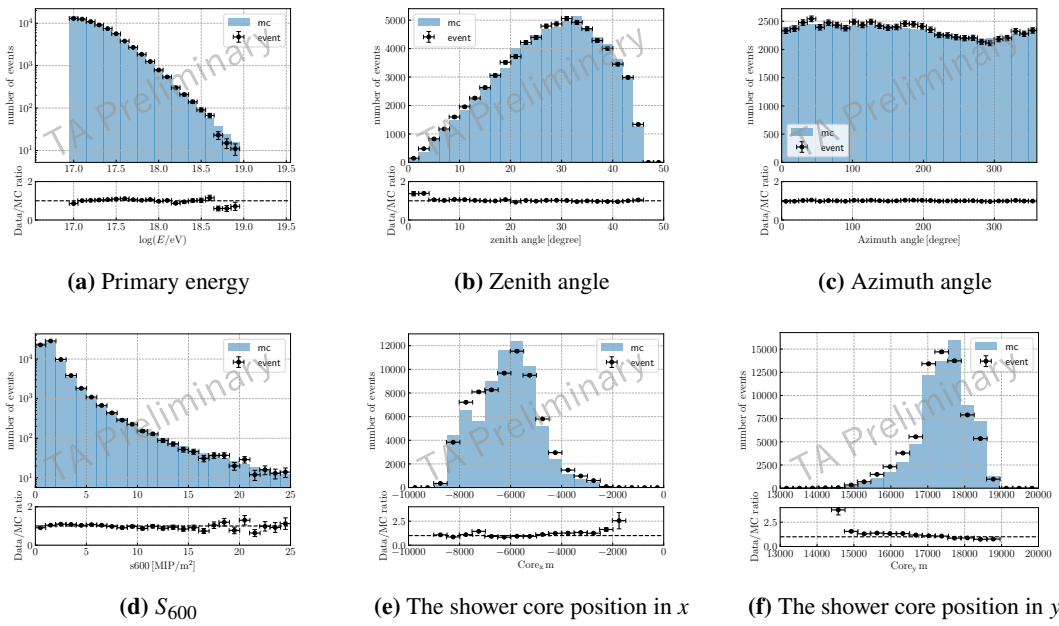


**Figure 7:** Data/Monte Carlo comparisons. The Monte Carlo simulation is a good representation of the data.

#### 4. Energy spectrum analysis with TALE-SD array

To obtain the energy spectrum, the exposures must first be calculated. The exposures cannot be calculated with a simple geometric factor because it depends on the performance of the surface detectors and also on the primary particles. Therefore, these dependencies are taken into account by the Monte Carlo simulations to estimate the aperture of the detector. In this analysis, the exposures were calculated under the assumption that the composition of primary cosmic rays is pure proton,

using the following equation:

$$\text{Exposure} = A_{\text{GEN}} \times \Omega_{\text{GEN}} \times \frac{N_{\text{REC}}^{\text{all cut}}}{N_{\text{GEN}}} \times T, \quad (4)$$

$$A_{\text{GEN}} = \pi \times 5.5^2 \text{ [km}^2\text{]}, \quad (5)$$

$$\Omega_{\text{GEN}} = \int_0^{2\pi} d\phi \int_{0^\circ}^{65^\circ} d\theta \sin \theta \cos \theta, \quad (6)$$

$$T = 1093 \text{ days}, \quad (7)$$

where  $A_{\text{GEN}} \times \Omega_{\text{GEN}}$  is the simulated aperture,  $N_{\text{REC}}^{\text{all cut}}$  is the number of reconstructed events,  $N_{\text{GEN}}$  is the number of simulated events and  $T$  is the number of days of data used in the analysis. The exposures calculated in this way are shown in Figure 8. The bins from  $10^{16.7}$  eV to  $10^{16.9}$  eV were not used in this analysis to remove the effect of migration from the lower bins.

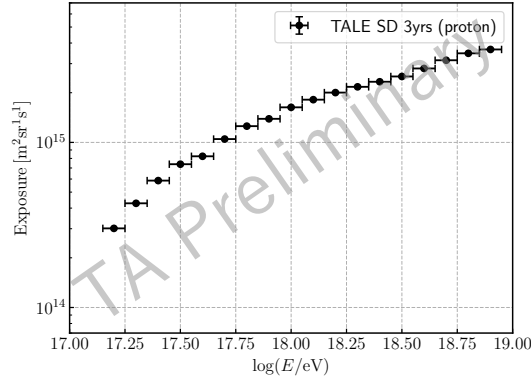


**Figure 8:** The exposure obtained by Monte Carlo simulation.

Figure 9a shows the energy histogram of events measured with the TALE-SD array. Dividing the value of each bin of this histogram by the value of the corresponding energy bin exposure and bin width yields the energy spectrum:

$$J = \frac{N(E)}{(\text{Exposure}) \cdot dE}. \quad (8)$$

The energy spectrum is shown in Figure 9b.

## 5. Conclusion

The TALE-SD array has been in operation since February 2018 with 80 SDs. The TALE-SD array DAQ is now running stably. The energy resolution is 25 % at  $10^{16.7}$  eV and 15 % at  $10^{18.9}$  eV, and the angular resolution is  $3^\circ$  at  $10^{16.7}$  eV and almost  $1^\circ$  at  $10^{18.9}$  eV. We compared the Monte Carlo and data and we have confirmed that they are consistent. And we evaluated the preliminary energy spectrum assuming a pure proton. In the future, we plan to obtain the energy estimation table, the exposure, and the energy spectrum that take into account the composition of cosmic rays.

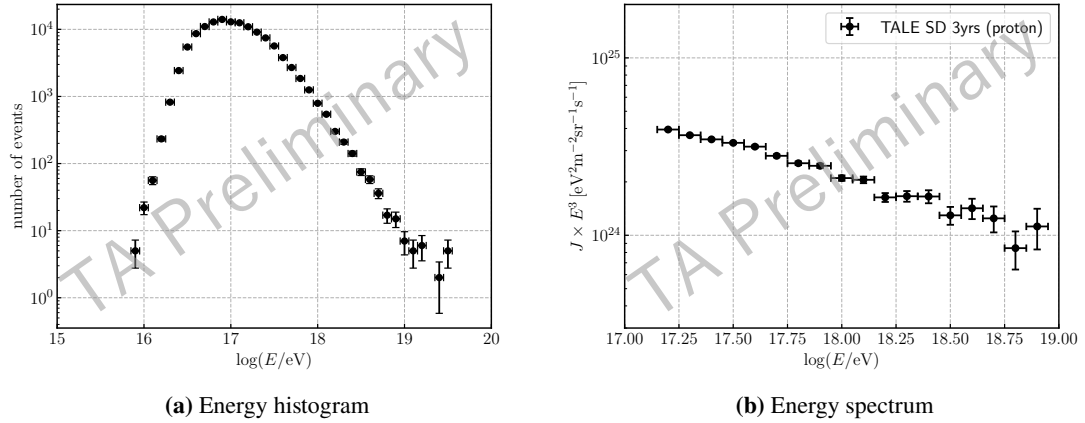


**Figure 9:** (a): The energy histogram of events measured with the TALE-SD array. (b): The energy spectrum from the actual data obtained by the TALE-SD array from October 2nd, 2019 to the end of September 28th, 2022.

## References

- [1] H. Kawai et al., *Nucl. Phys. B Proc. Suppl.* **175-176** (2008) 221.
- [2] T. Abu-Zayyad et al., *Nucl. Instrum. Methods Phys. Res. A* **689** (2012) 87.
- [3] H. Tokuno et al., *Nucl. Instrum. Methods Phys. Res. A* **676** (2012) 54.
- [4] R.U. Abbasi et al., *Astropart. Phys.* **68** (2015) 27
- [5] S. Ogio, *PoS ICRC2019* (2019) 375.
- [6] K. Sato, *PoS ICRC2019* (2019) 362.
- [7] J. Linsley and L. Scarsi *Phys. Rev.* **128** (1962) 2384.
- [8] T. Teshima et al., *J. Phys. G* **12** (1986) 1097.
- [9] S. Yoshida et al., *J. Phys. G* **20** (1994) 651.
- [10] H. Oshima et al., *EPJ Web Conf.* **283** (2023) 02006.
- [11] K. Fujita, Ph.D. thesis, Osaka City University (2022).
- [12] B.T. Stokes et al., *Astropart. Phys.* **35** (2012) 759.
- [13] S. Ostapchenko, *Phys. Rev. D* **83** (2011) 014018.
- [14] S. Agostinelli et al., *Nucl. Instrum. Methods Phys. Res. A* **506** (2003) 250.

## Full Authors List: the TelescopeArray Collaboration

R.U. Abbasi<sup>1</sup>, Y. Abe<sup>2</sup>, T. Abu-Zayyad<sup>1,3</sup>, M. Allen<sup>3</sup>, Y. Arai<sup>4</sup>, R. Arimura<sup>4</sup>, E. Barcikowski<sup>3</sup>, J.W. Belz<sup>3</sup>, D.R. Bergman<sup>3</sup>, S.A. Blake<sup>3</sup>, I. Buckland<sup>3</sup>, B.G. Cheon<sup>5</sup>, M. Chikawa<sup>6</sup>, A. Fedynitch<sup>6,7</sup>, T. Fujii<sup>4,8</sup>, K. Fujisue<sup>6</sup>, K. Fujita<sup>6</sup>, R. Fujiwara<sup>4</sup>, M. Fukushima<sup>6</sup>, G. Furlich<sup>3</sup>, Z. Gerber<sup>3</sup>, N. Globus<sup>9\*</sup>, W. Hanlon<sup>3</sup>, N. Hayashida<sup>10</sup>, H. He<sup>9</sup>, R. Hibi<sup>2</sup>, K. Hibino<sup>10</sup>, R. Higuchi<sup>9</sup>, K. Honda<sup>11</sup>, D. Ikeda<sup>10</sup>, N. Inoue<sup>12</sup>, T. Ishii<sup>11</sup>, H. Ito<sup>9</sup>, D. Ivanov<sup>3</sup>, A. Iwasaki<sup>4</sup>, H.M. Jeong<sup>13</sup>, S. Jeong<sup>13</sup>, C.C.H. Jui<sup>3</sup>, K. Kadota<sup>14</sup>, F. Kakimoto<sup>10</sup>, O. Kalashev<sup>15</sup>, K. Kasahara<sup>16</sup>, S. Kasami<sup>17</sup>, Y. Kawachi<sup>4</sup>, S. Kawakami<sup>4</sup>, K. Kawata<sup>6</sup>, I. Kharuk<sup>15</sup>, E. Kido<sup>9</sup>, H.B. Kim<sup>5</sup>, J.H. Kim<sup>3</sup>, J.H. Kim<sup>3†</sup>, S.W. Kim<sup>13</sup>, Y. Kimura<sup>4</sup>, I. Komae<sup>4</sup>, K. Komori<sup>17</sup>, Y. Kusumori<sup>17</sup>, M. Kuznetsov<sup>15,18</sup>, Y.J. Kwon<sup>19</sup>, K.H. Lee<sup>5</sup>, M.J. Lee<sup>13</sup>, B. Lubsandorzhev<sup>15</sup>, J.P. Lundquist<sup>3,20</sup>, T. Matsuyama<sup>4</sup>, J.A. Matthews<sup>3</sup>, J.N. Matthews<sup>3</sup>, R. Mayta<sup>4</sup>, K. Miyashita<sup>2</sup>, K. Mizuno<sup>2</sup>, M. Mori<sup>17</sup>, M. Murakami<sup>17</sup>, I. Myers<sup>3</sup>, S. Nagataki<sup>9</sup>, M. Nakahara<sup>4</sup>, K. Nakai<sup>4</sup>, T. Nakamura<sup>21</sup>, E. Nishio<sup>17</sup>, T. Nonaka<sup>6</sup>, S. Ogio<sup>6</sup>, H. Ohoka<sup>6</sup>, N. Okazaki<sup>6</sup>, Y. Oku<sup>17</sup>, T. Okuda<sup>22</sup>, Y. Omura<sup>4</sup>, M. Onishi<sup>6</sup>, M. Ono<sup>9</sup>, A. Oshima<sup>23</sup>, H. Oshima<sup>6</sup>, S. Ozawa<sup>24</sup>, I.H. Park<sup>13</sup>, K.Y. Park<sup>5</sup>, M. Potts<sup>3‡</sup>, M.S. Pshirkov<sup>15,25</sup>, J. Remington<sup>3</sup>, D.C. Rodriguez<sup>3</sup>, C. Rott<sup>3,13</sup>, G.I. Rubtsov<sup>15</sup>, D. Ryu<sup>26</sup>, H. Sagawa<sup>6</sup>, R. Saito<sup>2</sup>, N. Sakaki<sup>6</sup>, T. Sako<sup>6</sup>, N. Sakurai<sup>4</sup>, D. Sato<sup>2</sup>, K. Sato<sup>4</sup>, S. Sato<sup>17</sup>, K. Sekino<sup>6</sup>, P.D. Shah<sup>3</sup>, N. Shibata<sup>17</sup>, T. Shibata<sup>6</sup>, J. Shikita<sup>4</sup>, H. Shimodaira<sup>6</sup>, B.K. Shin<sup>26</sup>, H.S. Shin<sup>6</sup>, D. Shinto<sup>17</sup>, J.D. Smith<sup>3</sup>, P. Sokolsky<sup>3</sup>, B.T. Stokes<sup>3</sup>, T.A. Stroman<sup>3</sup>, Y. Takagi<sup>17</sup>, K. Takahashi<sup>6</sup>, M. Takamura<sup>27</sup>, M. Takeda<sup>6</sup>, R. Takeishi<sup>6</sup>, A. Taketa<sup>28</sup>, M. Takita<sup>6</sup>, Y. Tameda<sup>17</sup>, K. Tanaka<sup>29</sup>, M. Tanaka<sup>30</sup>, S.B. Thomas<sup>3</sup>, G.B. Thomson<sup>3</sup>, P. Tinyakov<sup>15,18</sup>, I. Tkachev<sup>15</sup>, H. Tokuno<sup>31</sup>, T. Tomida<sup>2</sup>, S. Troitsky<sup>15</sup>, R. Tsuda<sup>4</sup>, Y. Tsunesada<sup>4,8</sup>, S. Udo<sup>10</sup>, F. Urban<sup>32</sup>, I.A. Vaiman<sup>15</sup>, D. Warren<sup>9</sup>, T. Wong<sup>3</sup>, K. Yamazaki<sup>23</sup>, K. Yashiro<sup>27</sup>, F. Yoshida<sup>17</sup>, Y. Zhezher<sup>6,15</sup>, and Z. Zundel<sup>3</sup>

<sup>1</sup> Department of Physics, Loyola University Chicago, Chicago, Illinois 60660, USA

<sup>2</sup> Academic Assembly School of Science and Technology Institute of Engineering, Shinshu University, Nagano, Nagano 380-8554, Japan

<sup>3</sup> High Energy Astrophysics Institute and Department of Physics and Astronomy, University of Utah, Salt Lake City, Utah 84112-0830, USA

<sup>4</sup> Graduate School of Science, Osaka Metropolitan University, Sugimoto, Sumiyoshi, Osaka 558-8585, Japan

<sup>5</sup> Department of Physics and The Research Institute of Natural Science, Hanyang University, Seongdong-gu, Seoul 426-791, Korea

<sup>6</sup> Institute for Cosmic Ray Research, University of Tokyo, Kashiwa, Chiba 277-8582, Japan

<sup>7</sup> Institute of Physics, Academia Sinica, Taipei City 115201, Taiwan

<sup>8</sup> Nambu Yoichiro Institute of Theoretical and Experimental Physics, Osaka Metropolitan University, Sugimoto, Sumiyoshi, Osaka 558-8585, Japan

<sup>9</sup> Astrophysical Big Bang Laboratory, RIKEN, Wako, Saitama 351-0198, Japan

<sup>10</sup> Faculty of Engineering, Kanagawa University, Yokohama, Kanagawa 221-8686, Japan

<sup>11</sup> Interdisciplinary Graduate School of Medicine and Engineering, University of Yamanashi, Kofu, Yamanashi 400-8511, Japan

<sup>12</sup> The Graduate School of Science and Engineering, Saitama University, Saitama, Saitama 338-8570, Japan

<sup>13</sup> Department of Physics, Sungkyunkwan University, Jang-an-gu, Suwon 16419, Korea

<sup>14</sup> Department of Physics, Tokyo City University, Setagaya-ku, Tokyo 158-8557, Japan

<sup>15</sup> Institute for Nuclear Research of the Russian Academy of Sciences, Moscow 117312, Russia

<sup>16</sup> Faculty of Systems Engineering and Science, Shibaura Institute of Technology, Minato-ku, Tokyo 337-8570, Japan

<sup>17</sup> Graduate School of Engineering, Osaka Electro-Communication University, Neyagawa-shi, Osaka 572-8530, Japan

<sup>18</sup> Service de Physique Théorique, Université Libre de Bruxelles, Brussels, Belgium

<sup>19</sup> Department of Physics, Yonsei University, Seodaemun-gu, Seoul 120-749, Korea

<sup>20</sup> Center for Astrophysics and Cosmology, University of Nova Gorica, Nova Gorica 5297, Slovenia

<sup>21</sup> Faculty of Science, Kochi University, Kochi, Kochi 780-8520, Japan

<sup>22</sup> Department of Physical Sciences, Ritsumeikan University, Kusatsu, Shiga 525-8577, Japan

<sup>23</sup> College of Science and Engineering, Chubu University, Kasugai, Aichi 487-8501, Japan

<sup>24</sup> Quantum ICT Advanced Development Center, National Institute for Information and Communications Technology, Koganei, Tokyo 184-8795, Japan

<sup>25</sup> Sternberg Astronomical Institute, Moscow M.V. Lomonosov State University, Moscow 119991, Russia

<sup>26</sup> Department of Physics, School of Natural Sciences, Ulsan National Institute of Science and Technology, UNIST-gil, Ulsan 689-798, Korea

<sup>27</sup> Department of Physics, Tokyo University of Science, Noda, Chiba 162-8601, Japan

<sup>28</sup> Earthquake Research Institute, University of Tokyo, Bunkyo-ku, Tokyo 277-8582, Japan

<sup>29</sup> Graduate School of Information Sciences, Hiroshima City University, Hiroshima, Hiroshima 731-3194, Japan

<sup>30</sup> Institute of Particle and Nuclear Studies, KEK, Tsukuba, Ibaraki 305-0801, Japan

<sup>31</sup> Graduate School of Science and Engineering, Tokyo Institute of Technology, Meguro, Tokyo 152-8550, Japan

<sup>32</sup> CEICO, Institute of Physics, Czech Academy of Sciences, Prague 182 21, Czech Republic

## Acknowledgment

The Telescope Array experiment is supported by the Japan Society for the Promotion of Science(JSPS) through Grants-in-Aid for Priority Area 431, for Specially Promoted Research JP21000002, for Scientific Research (S) JP19104006, for Specially Promoted Research JP15H05693, for Scientific Research (S) JP19H05607, for Scientific Research (S) JP15H05741, for Science Research (A) JP18H03705, for Young Scientists (A)

\* Presently at: University of California - Santa Cruz

† Presently at: Argonne National Laboratory, Physics Division, Lemont, Illinois 60439,USA

‡ Presently at: Georgia Institute of Technology, Physics Department, Atlanta, Georgia 30332,USA

JPH26707011, and for Fostering Joint International Research (B) JP19KK0074, by the joint research program of the Institute for Cosmic Ray Research (ICRR), The University of Tokyo; by the Pioneering Program of RIKEN for the Evolution of Matter in the Universe (r-EMU); by the U.S. National Science Foundation awards PHY1607727, PHY-1712517, PHY-1806797, PHY-2012934, and PHY-2112904; by the National Research Foundation of Korea (2017K1A4A3015188, 2020R1A2C1008230, & 2020R1A2C2102800); by the Ministry of Science and Higher Education of the Russian Federation under the contract 075-15-2020-778, IISN project No. 4.4501.18, and Belgian Science Policy under IUAP VII/37 (ULB). This work was partially supported by the grants of The joint research program of the Institute for Space-Earth Environmental Research, Nagoya University and Inter-University Research Program of the Institute for Cosmic Ray Research of University of Tokyo. The foundations of Dr. Ezekiel R. and Edna Wattis Dumke, Willard L. Eccles, and George S. and Dolores Doré Eccles all helped with generous donations. The State of Utah supported the project through its Economic Development Board, and the University of Utah through the Office of the Vice President for Research. The experimental site became available through the cooperation of the Utah School and Institutional Trust Lands Administration (SITLA), U.S. Bureau of Land Management (BLM), and the U.S. Air Force. We appreciate the assistance of the State of Utah and Fillmore offices of the BLM in crafting the Plan of Development for the site. Patrick A. Shea assisted the collaboration with valuable advice and supported the collaborations efforts. The people and the officials of Millard County, Utah have been a source of steadfast and warm support for our work which we greatly appreciate. We are indebted to the Millard County Road Department for their efforts to maintain and clear the roads which get us to our sites. We gratefully acknowledge the contribution from the technical staffs of our home institutions. An allocation of computer time from the Center for High Performance Computing at the University of Utah is gratefully acknowledged.